Natural and Mining-Related Sulfate Sources at Two High-Sulfidation Deposits Constrained by a Triple-Tracer Bayesian Isotope Mixing Model

Camilo Raúl de los Hoyos[1], Claudina González[1], Juana María Canavessi[1], Matthew Leybourne[2], Daniel Layton-Matthews[2], Alejandro Verri Kozlowski[1], Robert Bowell[3]

[1]*SRK Consulting (Argentina) S.A., Salta, Argentina, cdeloshoyos@srk.com.ar*

[2]*Queen's Facility for Isotope Research, Kingston, Canada*

[3]*SRK Consulting (UK) Ltd., Cardiff, Wales*

Abstract

Distinguishing natural from mining-derived sulfate in surface water is particularly challenging in high-altitude catchments hosted in intensely hydrothermally altered lithologies. Two compliance monitoring stations downstream of two high-sulfidation epithermal deposits (VD and PL) were investigated using a triple-tracer Bayesian isotope mixing model (δ^{34}SSO4, δ^{18}OSO4, δ^{18}Owater; MixSIAR). Natural hydrothermal and geothermal sources dominate sulfate loading at both stations: at TAG_mid (VD), DPB and TAG_sup account for ~66% of the sulfate budget, with mining-related contributions (~8%) smaller than the unaccounted source fraction. At TAG_low (PL), the upstream TAG_mid reach contributes ~74%, propagating the predominantly natural signal downstream. In contrast to sulfate, dissolved As decreases ~600-fold between TAG_mid and TAG_low, while total As loads remain near-conservative (~4.5% decrease), indicating phase transfer to the particulate fraction through Fe-hydroxide co-precipitation induced by lime treatment rather than mass removal from the system.

Keywords: Sulfate source proportions, stable isotopes, Bayesian isotope mixing, high-sulfidation

Introduction

Characterizing sources of sulfate, arsenic (As), and potentially toxic metals is essential for accurate water quality monitoring, regulatory compliance, and remediation. Distinguishing anthropogenic from natural sulfate sources in catchments associated with high-sulfidation epithermal mine sites is challenging, as natural weathering of sulfur-bearing minerals in hydrothermal alteration zones produces hydrochemical signatures similar to those from mining activities. Sulfur and oxygen stable isotopes (δ^{34}S and δ^{18}OSO4) provide a useful tool for assessing sulfate source contributions (e.g., Pellicori *et al.*, 2005). Combined with hydrochemical data and Bayesian mixing models, this multi-tracer approach offers a robust statistical framework for quantifying source proportions with full uncertainty characterization (Stock *et al.*, 2018; Zhang *et al.*, 2024).

This study focuses on the origin of sulfate in surface water at two compliance monitoring stations, located downstream of two high-sulfidation epithermal deposits (hereinafter VD and PL; site identities and operational details are withheld under a non-disclosure agreement between SRK and the Client).

Methods

Hydrochemical characterisation and sulfate load estimations drew on the client's monitoring database (>20 years), with a baseline period from 1999/2000 until 2004. Water samples were analyzed for stable isotopes and dissolved constituents. δ^{18}Owater and δ^{2}H were measured by IRMS (CO_2 equilibration and thermo-chemical reduction, respectively; VSMOW reference). δ^{34}S and δ^{18}OSO4 were determined after $BaSO_4$ precipitation by IRMS (VCDT and VSMOW references). Analytical precision: ±0.2‰ for δ^{18}O and δ^{34}S; ±3‰

for δ^2H. Major anions were measured by ion chromatography; major and trace cations by ICP-MS.

Bayesian mixing models were implemented in MixSIAR v3.1 (Stock *et al.* 2018) using three simultaneous tracers ($\delta^{34}S$, $\delta^{18}OSO4$, $\delta^{18}Owater$). Concentration-dependent mixing was applied using sulfate as the weighting variable. Informative priors were constructed from log_{10}-transformed sulfate mass loads per source (prior strength = 1.5). Sensitivity to prior specification was evaluated against a uniform prior. Markov Chain Monte Carlo (MCMC) convergence was assessed with the Gelman-Rubin diagnostic ($\hat{R} < 1.1$).

Site, sources and mixtures characterisation

Geological, and hydrochemical setting

The study area occupies a high-altitude mountainous region (4,000–5,000 m.a.s.l.) spanning two Köppen climate zones: cold arid steppe (BSk) and polar tundra (ET). Precipitation is scarce and predominantly in the form of snowfall during winter; surface runoff is consequently driven by snowmelt, with peak streamflow occurring between October and February.

VD is a high-sulfidation epithermal deposit that is almost completely oxidized. The district lithology comprises felsic intrusive bodies (granites and monzonites) at the margins, andesitic rocks and volcanic breccias in the interior, and rhyolites within the open pit areas. Hydrothermal alteration is intense and pervasively zoned. Silicic cores bearing jarosite and alunite correspond to the mineralized zones and are surrounded by advanced argillic assemblages, with distal propylitic alteration (chlorite–epidote) developed at the outer margins. Gold is associated with iron oxides (hematite and goethite) and jarosite, whereas hypogene sulfides are rare or absent.

PL is a high-sulfidation epithermal deposit dominated by primary hypogene mineralization. Lithology is dominated by porphyritic granite and dacitic porphyry, with felsic tuffs at the margins and diorite stocks intruding the sequence. Hydrothermal alteration is pervasive and multistage. Silicic alteration (vuggy quartz) characterizes the mineralized breccia cores, which are surrounded by advanced argillic assemblages, with distal propylitic alteration at the outer margins. Gold and silver are primarily hosted within a hypogene alunite–pyrite–enargite assemblage, occurring as trace constituents within the enargite and pyrite structure.

Surface water chemistry is strongly controlled by the hydrothermal alteration zones within each sub-catchment. Waters draining silicic and advanced argillic zones are naturally acidic and sulfate-rich, enriched in aluminum and trace metals, with jarosite dissolution as the primary natural source of acidity in VD and PL, the latter involving pyrite oxidation. Catchments influenced by propylitic alteration (source PT) produce Ca-SO_4-type waters at near-neutral pH, while sectors draining unaltered primary volcanic lithologies yield Na–Cl signatures. The geothermal system southeast of the project represents the dominant natural sulfate and As to the downstream monitoring points (source DPB). Contribution from groundwater and minor springs was not considered in this study.

Sources and mixture sites

Sources were characterized from water samples collected during three field campaigns to capture temporal variability, whereas solid-phase isotopic data for alunite and jarosite were compiled from the literature (Deyell *et al.*, 2005; Holley *et al.*, 2017). All sources and mixing sites are summarized in Table 1 and Figure 2. For VD, five sources were defined: three natural – geothermal spring tributary DPB, upper main collector TAG_sup, and the sub-catchment PT – and two mining-related: the Valley Leach Facility (VLF) and the Open Pit (OP). Contribution assessment from VLF and OP was included using a highly conservative approach: fixed flow rates of 7 L/s (VLF) and 10 L/s (OP) were assigned to represent hypothetical seepage scenarios. This intentionally biases the model toward maximizing mining-related inputs. For PL, four sources were characterized: one predominantly natural upstream source, TAG_mid; one natural acid rock drainage source, Turbio_head which also includes groundwater originating from the tunnel (pH ~3.3; $\delta^{34}S$ = −0.7‰) that is captured

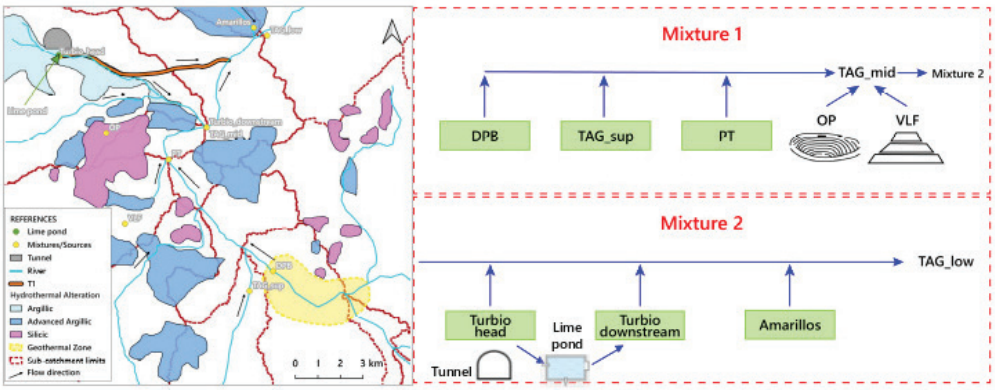

Figure 1 *Sketch map of hydrothermal alteration zones (a) and sources-mixtures scheme (b).*

and conveyed through a pipe system (T1 in Figure 1) and discharged near TAG_low; one partially mining-influenced source, Turbio_downstream, which consists of lime-treated drainage from a mining tunnel intercepting the Turbio_head aquifer, supplemented by minor natural tributaries; and one natural drainage from the PL argillic alteration zone, Amarillos ($\delta^{34}S$ = −5.4‰). Despite both Turbio_head and Amarillos being sourced from the PL alteration zone, their contrasting isotopic signatures likely reflect different alteration assemblages or sulfide oxidation pathways (Deyell *et al.*, 2005). The heavier $\delta^{34}S$ of Turbio_downstream relative to Turbio_head may reflect kinetic fractionation during lime-induced gypsum precipitation. Table 1 combines data from high- and low-flow campaigns; seasonal disaggregation was beyond the scope of this study but would allow identification of gaining and losing reaches and is recommended for future work.

Results and discussion

Isotopic mixing space for sources and mixtures and model results

The $\delta^{34}S$ vs. $\delta^{18}OSO4$ biplots (Figure 2a and c) suggest differentiation among sources at both sites. At VD, solid-phase analyses define two distinct mineral fields: VD_jar ($\delta^{34}S$: −3.8 to −0.8‰; $\delta^{18}O\text{-}SO_4$: −4 to +0.7‰) and VD_aln ($\delta^{34}S$: +5.9 to +17.5‰; $\delta^{18}OSO4$: +2 to +9‰), separated by ~15‰ in $\delta^{34}S$ and consistent with the contrasting formation mechanisms of these phases (Deyell *et al.*, 2005). $\delta^{34}S$ values for VLF are similar to those for VD_jar, suggesting jarosite dissolution as a plausible sulfate source by dissolution. OP shows broader scatter although closer to VD_aln field, suggesting predominance of alunite mineralogy of the pit walls; the highest $\delta^{34}S$ sample (~12.9‰) plots to VD_aln, likely reflecting dominant alunite dissolution at that sampling station. The $\delta^{34}S$ vs. $\delta^{18}OSO4$ (Figure 2c) shows some overlapping between DPB and OP, although both sources plot clearly distinguished within the mixing space $\delta^{34}S$ vs. $\delta^{18}Owater$ (Figure 2b).

At PL, the PL_py $\delta^{34}S$ range (−6 to −3.4‰) plots towards the lightest portion of the system (Figure 2c). Amarillos is clearly distinguished in the $\delta^{34}S$ vs. $\delta^{18}OSO4$ biplot, and plots within the PL_py $\delta^{34}S$ range. Turbio_head tends to plot towards PL_jar $\delta^{34}S$ range. TAG_mid (which is now a source) is plotted almost together with TAG_low (mixture) both in the $\delta^{34}S$ vs. $\delta^{18}OSO4$ and the $\delta^{34}S$ vs. $\delta^{18}Owater$ mixing spaces (Figure 2d). The PL_aln field ($\delta^{34}S$ = +12.6 to +24.5‰; $\delta^{18}OSO4$ = +13.8–+20.7‰) lies entirely outside the PL mixing space, indicating that alunite dissolution does not constitute an important dissolved sulfate source at this monitoring station (TAG_low) under sampled conditions. All VD and PL samples plot within the isotope mixing space of their respective end-member sets, validating the source framework.

MCMC convergence was confirmed, with $\hat{R} < 1.1$ for all modeled parameters. Sensitivity analysis showed differences between informative and uniform prior models for all

Table 1 Isotopic composition (mean ± 1SD) and classification of end-members and mixing sites. pH values are averaged. Sulfate and As are dissolved contents. n = number of isotope results.

Source/Mixture	pH	$\delta^{34}S_{SO4}$ (‰)	$\delta^{18}O_{SO4}$ (‰)	$\delta^{18}O_{water}$ (‰)	Sulfate (mg/L)	As[1] (µg/L)	Flow (L/s)
VD sources							
DPB (n = 7)	7.6	3.8 ± 1.1	2.2 ± 1.4	−15.6 ± 0.7	299 ± 72	1479 ± 455	583 ± 406
TAG_sup (n = 6)	8.1	2.6 ± 0.6	1.1 ± 1.2	−16.0 ± 0.5	706 ± 7	489 ± 574	325 ± 236
PT (n = 9)	9	1.5 ± 0.6	0.2 ± 0.9	−17.0 ± 0.4	397 ± 15	66 ± 78	35 ± 41
VLF (n =4)	10.1	−1.2 ± 1.4	3.0 ± 1.0	−15.8 ± 1.3	1060 ± 26	348 ± 35	7 ± 1
OP (n = 13)	3.4	4.3 ± 3.4	3.9 ± 1.5	−17.9 ± 0.6	28 ± 3	0.63 ± 0.62	10 ± 1
TAG_mid (n = 4)	8.1	2.3 ± 0.4	0.6 ± 1.2	−15.8 ± 0.5	500 ± 45	813 ± 328	969 ± 615
PL sources							
TAG_mid (n = 4)	8.1	2.0 ± 0.6	0.7 ± 1.1	−15.8 ± 0.4	500 ± 45	813 ± 328	969 ± 615
Turbio_head (n = 6)	3.3	−0.7 ± 1.3	−0.5 ± 1.9	−16.7 ± 1.1	2600 ± 1570	224 ± 181	59 ± 66
Turbio_downstream (n = 6)	4.1	2.9 ± 1.0	−0.7 ± 1.5	−16.7 ± 0.3	895 ± 34	0.45 ± 0.24	122 ± 70
Amarillos (n = 6)	4.9	−5.4 ± 0.8	−7.3 ± 1.6	−16.4 ± 0.2	805 ± 317	0.78 ± 1.03	126 ± 105
TAG_low (n = 6)	5.1	1.6 ± 0.6	−0.9 ± 1.4	−15.6 ± 0.2	704 ± 27	1.26 ± 2.75	1141 ± 745

[1]Arsenic contents are reported in µg/L, given their low values relative to sulfate and their wide variability across sources.

sources of less than 15% for VD and less than 5% for PL, indicating that the three-tracer isotopic system carries sufficient information to constrain the posteriors without excessive dependence on the prior.

Source proportional contribution at VD

Natural sources dominate sulfate at TAG_mid (Fig. 3a). TAG_sup and DPB are the main contributors (~66% combined posterior median; 95% credible interval or CI), reflecting the substantial hydrothermal sulfate background characteristic of high-sulfidation systems. PT contributes ~19%, acting mainly as a dilution end-member. Mining contributions from VLF and OP are 4.9% and 2.9% respectively (~8% combined), smaller than the unaccounted fraction of 6.5% (100% - Σsource-proportions), even though assigned sulfate loads were highly conservative. Wide CIs reflect uncertainty inherent to a five-source system with n = 4 mixture samples. Predicted sulfate concentrations agree reasonably with observed values at TAG_mid.

Source proportional contribution at PL

TAG_mid is the dominant source at TAG_low (~74% posterior median; 95% CI; Fig. 3b), robust to prior specification and reflecting the physical dominance of the main river collector. Since TAG_mid is predominantly natural, a strong natural signature propagates to TAG_low. Turbio_head and Turbio_downstream contribute ~16% combined, where Turbio_downstream (~8.8%) represents a partially mining-related pathway to TAG_low. Amarillos, the isotopically most distinguishable source, contributes ~6%. Overall mining influence is small relative to the natural geothermal and hydrothermal background. TAG_mid remains distinguishable as the dominant source, with a lower credible limit (~27%) exceeding the medians of all other sources. Credible intervals are wide for TAG_mid and Turbio_head, reflecting inherent uncertainty due to the limited number of samples in the mixture (n=6). The predicted sulfate concentration at TAG_low (~950 mg/L) exceeds measured contents (~700 mg/L), suggesting active sulfate removal in the confluence and consistent with gypsum precipitation when Ca^{2+}-rich lime-treated water from Turbio_downstream contacts the sulfate-rich TAG_mid water, a process supported by the isotopic fractionation observed in Turbio_downstream.

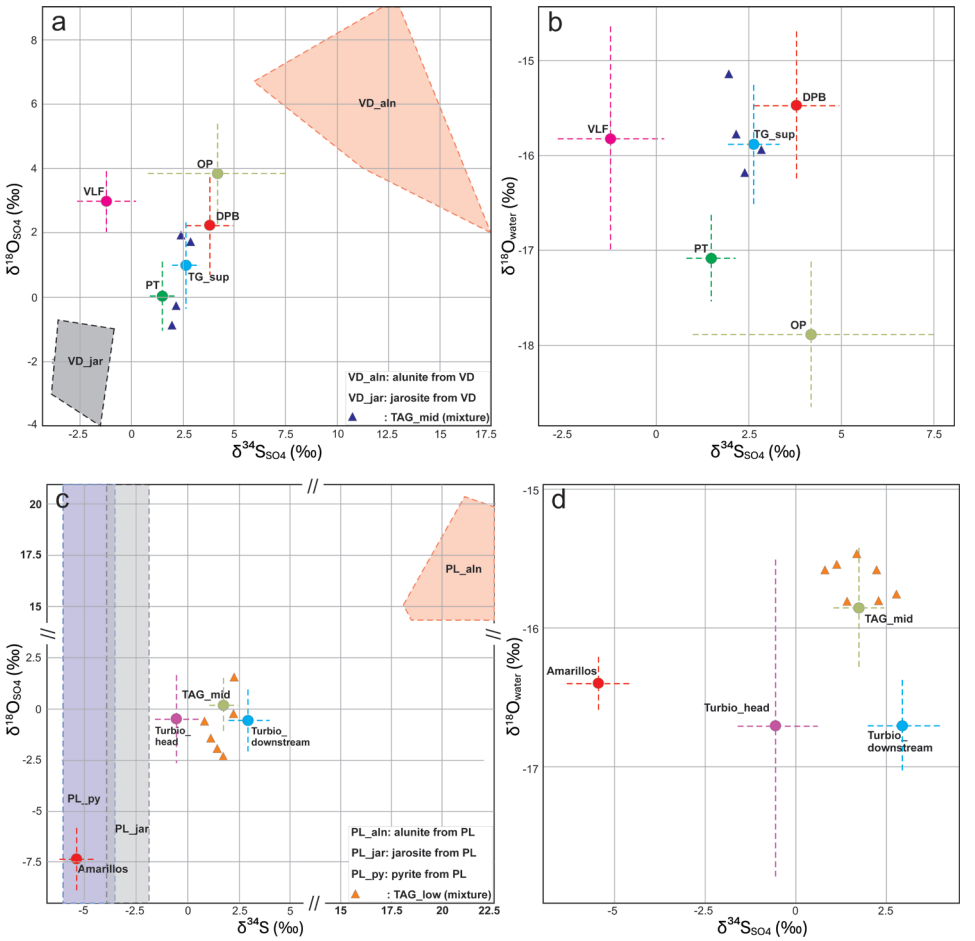

Figure 2 *Biplots for the triple-tracer $\delta^{34}S$ – $\delta^{18}O_{SO4}$ – $\delta^{18}O_{water}$ system including sources, mixtures and solid-phase isotopic signatures for VD (a and b) and PL (c and d).*

Dissolved arsenic non-conservativity between TAG_mid and TAG_low

The most notable feature of the TAG_mid–TAG_low segment is the behavior of As. Dissolved As shows strongly non-conservative behavior between the two compliance stations (Table 1). At TAG_mid (pH 8.1), dissolved As averages 813 ± 328 µg/L, dominated by the geothermal source DPB (1,479 ± 455 µg/L at pH 7.6), while mining-related sources contribute negligibly. Total As at TAG_mid averages 1,289 µg/L, indicating that ~37% of As is already particulate at this station, likely associated with Fe and Al hydroxide colloids stable at near-neutral pH.

At TAG_low (pH 5.1), dissolved As drops to 1.26 ± 2.75 µg/L, which is a ~600-fold decrease relative to TAG_mid, while total As remains at 1,045 µg/L, implying that >99% of As at TAG_low is particulate. Total As loads are near-conservative between stations (TAG_mid: ~1,249,000 µg/s; TAG_low: ~1,192,000 µg/s; ~4.5% difference), suggesting that this decrease does not represent mass removal but rather phase change to the particulate fraction, likely through adsorption onto Fe-hydroxide flocs. The contrast between Turbio_head (224 ± 181 µg/L; pH 3.3) and Turbio_downstream (0.45 ± 0.24 µg/L; pH 4.1) suggests that lime treatment efficiently removes great part of the dissolved As prior to confluence. Thus, the decrease in dissolved As (V) between TAG_mid and TAG_low may rather represent adsorption

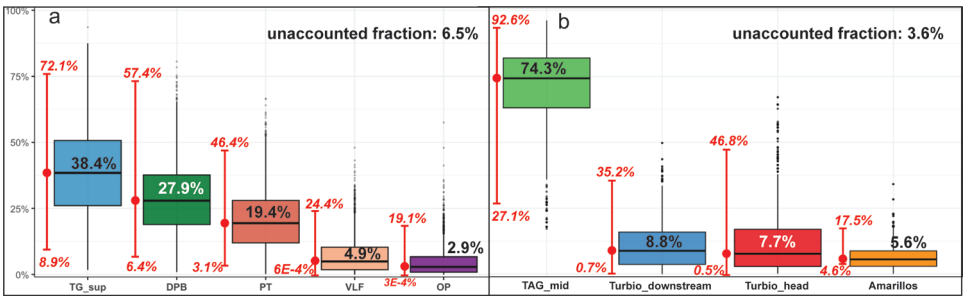

Figure 3 Boxplots of source contributions at VD (a) and PL (b). Median values are indicated within the boxplots. 95% credible intervals (2.5 to 97.5% CI) are shown in red to the left of each boxplot, with red points indicating the position of the median.

onto Fe-hydroxide flocs generated by lime treatment in the Turbio_downstream source. Speciation of As was not considered in this study, although it is strongly recommended for future work.

Conclusions

Sulfate load proportions were estimated considering combined high-flow and low-flow conditions. A triple-tracer Bayesian isotope mixing approach successfully quantified sulfate source contributions, in terms of mass, at two compliance monitoring sites within high-sulfidation epithermal catchments. At TAG_mid (VD), hydrothermal inputs (DPB and TAG_sup) dominate the sulfate budget (~66%), with PT acting primarily as a dilution source; mining-related contributions from the OP and VLF are quantifiable but minor (~8%), smaller than the unaccounted source fraction. At TAG_low (PL), upstream inputs dominate (~74% from TAG_mid); the Turbio system accounts for ~16% of the sulfate load, with Turbio_downstream as the primary mining-related pathway. In both cases, the sulfate budget is predominantly controlled by natural hydrothermal sources.

In contrast to sulfate, dissolved As shows non-conservative behavior along the TAG_mid–TAG_low segment. Total As loads are near-conservative (~4.5% decrease), whereas dissolved As decreases ~600-fold, suggesting phase transfer to the particulate fraction through Fe-hydroxide co-precipitation induced by lime treatment rather than removal from the system.

These results have direct implications for environmental monitoring in high-sulfidation deposits, where sulfate concentrations may be predominantly natural and might be misattributed to mining environmental affectation. The combined use of multiple isotopic tracers and Bayesian mixing models provides a robust and transferable framework for source apportionment in complex systems, particularly where overlapping source signatures and non-conservative behavior may complicate interpretation.

References

Deyell, C.L., Rye, R.O., Landis, G.P. & Bissig, T. (2005). Alunite and the role of magmatic fluids in the Tambo high-sulfidation deposit, El Indio–Pascua belt, Chile. Chemical Geology, 215, 185–218.

Holley, E.A., Monecke, T., Bissig, T., & Reynolds, J. (2017). Evolution of High-Level Magmatic-Hydrothermal Systems: New Insights from Ore Paragenesis of the Veladero High-Sulfidation Epithermal Au-Ag Deposit, El Indio-Pascua Belt, Argentina. Economic Geology, 112, 1747-1771.

Pellicori, D.A., Gammons, C.H. & Poulson, S.R. (2005). Geochemistry and stable isotope composition of the Berkeley pit lake and surrounding mine waters, Butte, Montana. Applied Geochemistry, 20, 2116–2137.

Smedley, P.L. & Kinniburgh, D.G. (2002). A review of the source, behaviour and distribution of arsenic in natural waters. Applied Geochemistry, 17, 517–568.

Stock, B.C., Jackson, A.L., Ward, E.J., Parnell, A.C., Phillips, D.L. & Semmens, B.X. (2018). Analyzing mixing systems using a new generation of Bayesian tracer mixing models. PeerJ, 6, e5096.

Zhang, K.; Shi, Z.; Ding, X.; Ge, L.; Xiong, M.; Zhang, Q.; Lai, W.; Ge, L (2024). Identification of Anthropogenic and Natural Inputs of Sulfate into River System of Carbonate Zn-Pb Mining Area in Southwest China: Evidence from Hydrochemical Composition, δ34SSO4 and δ18OSO4. Water 2024, 16, 2311.